International Journal of Production Research

ISSN: 0020-7543 (Print) 1366-588X (Online) Journal homepage: http://www.tandfonline.com/loi/tprs20

Modelling and joint monitoring of input and output of systems with arbitrary order autoregressive disturbance

Shichang Du & Rui Zhang

To cite this article: Shichang Du & Rui Zhang (2016) Modelling and joint monitoring of input and output of systems with arbitrary order autoregressive disturbance, International Journal of Production Research, 54:6, 1822-1838, DOI: 10.1080/00207543.2015.1078921

To link to this article: http://dx.doi.org/10.1080/00207543.2015.1078921

International Journal of Production Research, 2016
Vol. 54, No. 6, 1822–1838, http://dx.doi.org/10.1080/00207543.2015.1078921

Taylor & Francis
Taylor & Francis Group

Modelling and joint monitoring of input and output of systems with arbitrary order autoregressive disturbance

Shichang Du[a,b]* and Rui Zhang[b]

[a]*State Key Lab of Mechanical System and Vibration, Shanghai Jiaotong University, Shanghai, P.R. China;* [b]*Department of Industrial Engineering and Management, School of Mechanical Engineering, Shanghai Jiaotong University, Shanghai, P.R. China*

(*Received 12 January 2015; accepted 22 July 2015*)

Considerable studies have been done on modelling and joint monitoring of input and output of systems with autoregressive moving average (ARMA) disturbance. Most of these studies focus on systems with ARMA (1, 1) disturbance. However, many kinds of systems are not conform to ARMA(1, 1) disturbance. Motivated by the fact that an autoregressive (AR) model with high order can be implemented to approximate the stationary ARMA model at any precision, a new generic model and a joint monitoring scheme of systems with arbitrary order AR(p) disturbance are developed. A minimum mean squared error (MMSE) controller with arbitrary order AR disturbance is designed to reduce the system variability. The mathematical expectation and average run length of MMSE-controlled outputs are derived. A new joint chart for monitoring the input and output simultaneously is explored. Two out-of-control rules for the joint monitoring chart are developed. The monitoring performances of the input chart, the output chart and the joint monitoring chart are also discussed. The results of simulation experiments and case studies validate the effectiveness of the developed model and joint monitoring chart.

Keywords: autoregressive disturbance; MMSE controller; joint monitoring; statistical process control; engineering process control

1. Introduction

The ability to reduce system variation for quality control and productivity improvement in manufacturing and service systems plays an essential role in the success of enterprises in today's globally competitive marketplace (Du et al. 2008; Montgomery 2009). Amongst various techniques applied to reduce system variation and achieve system stability, statistical process control (SPC) and engineering process control (EPC) are two powerful tools that are widely used in manufacturing and service systems. Montgomery et al. (1994) pointed out that the SPC and EPC integration model is effective to the process monitoring and adjustment and that proper employing both SPC and EPC can always outperform the application of either alone. The integration of SPC and EPC has attracted lots of attentions from both academia and industry (e.g. Messina et al. 1996; Jiang and Tsui 2002; Park et al. 2012). However, there is an adverse impact called as the limited 'window of opportunity' in the integrated area (Vander Wiel 1996). Window of opportunity is a short interval immediately after the occurrence of a special cause within which a signal can be detected (Wang and Tsung 2007). Once a special cause occurs, the feedback controller can immediately compensate process outputs, which will result in that the SPC chart is difficult to perceive the special cause. Therefore, the SPC chart will not have an excellent monitoring performance, if its monitoring object is only process outputs without consideration of manipulated inputs.

Because manipulated inputs can reflect the occurrence status of process faults, Messina et al. (1996) studied the monitoring of manipulated inputs for a minimum mean squared error (MMSE)-controlled process under an autoregressive moving average (ARMA) disturbance model. Tsung, Shi, and Wu (1999) and Tsung and Shi (1999) developed the joint chart to simultaneously monitoring Proportional-Integral-Derivative (PID)-controlled outputs and control actions. Similarly, Jiang and Tsui (2002) compared monitoring performances of the process output and the control action of MMSE- and Proportional-Integral (PI)-controlled ARMA(1, 1) processes, respectively. It was found that under a large mean shift, monitoring the process output is always more efficient than monitoring the manipulated variable; under a small mean shift, when $\phi < 0$ (ϕ is process parameter), it is consistent with the preceding conclusion; while it is in contrast to the preceding conclusion when $\phi > 0$. Jiang (2004) proposed a joint monitoring scheme which combines the data

*Corresponding author. Email: lovbin@sjtu.edu.cn

streams of process outputs and manipulated inputs based on a uniformly most powerful test. The scheme can be adjusted to be sensitive to large or small shifts.

However, all of the current joint charts are based on ARMA(1, 1) disturbance model, and there is no research on dealing with the processes under arbitrary order disturbance models. Many kinds of production processes are not conformed to the ARMA(1, 1) disturbance model. For example, an autoregressive AR(4) model is appropriate for a mechanical system consisting of a mass, a dashpot and a spring, and an AR(6) model is used to fit the micrometre readings of two diameters on the same machined part (Pandit and Wu 1983). A series consisting of 226 temperature readings are fitted as an AR(3) model (Peña, Tiao, and Tsay 2011). An aircraft horizontal stabiliser assembly process of 2781 product data is fitted as an AR(5) model (Du and Xi 2010, 2011). A valve shell machining process is fitted as an AR(6) model (Du, Yao, and Huang 2015). More examples about high-order processes can be found in Bowerman and O'Connell (1993) and Brockwell and Davis (2002). This effort is motivated by the fact that an AR(p) model can implement approximating the stationary ARMA model at any precision. The main contribution of this study is that a new joint monitoring scheme of processes with arbitrary order AR(p) disturbance is developed.

The remainder of this study is organised as follows. The process model of the linear dynamic feedback is proposed and an MMSE controller is designed in Section 2. The mathematical expectation and the average run length (ARL) of MMSE-controlled outputs are derived in Section 3. The joint chart is designed, its out-of-control rules are developed and its performance analysis is presented in Section 4. Case studies are conducted in Section 5. Finally, conclusions are given in Section 6.

2. MMSE-controlled process model

The MMSE controller and the PID controller are two common EPC controllers in industrial practice. The PID controller is more robust than the MMSE controller with regard to disturbance model uncertainty when the model parameter is incorrectly estimated (Tsung, Wu, and Nair 1998). However, MMSE-controlled outputs are independent identical distribution (IID), that is, MMSE controller can eliminate the autocorrelation of process outputs. Besides, the MMSE scheme can minimise the mean squared error (MSE), so the control performance of MSE of the PID controller is always inferior to that of the MMSE controller. Therefore, for the convenience of the research on the AR(p) process, it is assumed that the process can be accurately estimated. This study focuses on the MMSE-controlled processes and the output of the process can be reduced to a white noise by the MMSE controller.

Let e_t denote the process output at instant t, X_t manipulated variable and its initial value $X_0 = 0$, D_t the process disturbance, μ_t the mean shift and B the backward shift operator. Without loss of generality, assume the target value of the process output is zero. Because the output from the process dynamics $Y_t = X_{t-1}$ in the most of discrete part manufacturing systems, the process output e_t can be defined as:

$$e_t = Y_t + D_t + \mu_t = X_{t-1} + D_t + \mu_t \tag{1}$$

It is noteworthy that the process disturbance D_t needs a specific time series model. Vander Wiel (1996) used the first-order integrated moving average (IMA(0, 1, 1)) model to study the process monitoring. Box, Tiao, and Bisgaard (2000) emphasised the use of non-stationary models, including the IMA(0, 1, 1) model. Meanwhile, because most of process disturbances can be modelled as stationary processes, Tsung and Shi (1999), Jiang and Tsui (2002) and Jiang (2004) all used a stationary ARMA(1, 1) model to study the monitoring of process outputs and control actions. However, the high-order time series models have not been widely studied so that the applicable scope of the joint monitoring chart is restricted. Therefore, this study assumes D_t as a stationary AR(p) process, i.e.:

$$D_t = \varphi_1 D_{t-1} + \varphi_2 D_{t-2} + \cdots + \varphi_p D_{t-p} + a_t = \frac{1}{1 - \varphi_1 B - \cdots - \varphi_p B^p} a_t \tag{2}$$

where $\varphi_1, \varphi_2, \ldots, \varphi_p$ represent process parameters, and a_t represents a white noise variable with an in-control mean of zero and variance σ_a^2.

There exists no mean shifts under a normal in-control process, i.e. $\mu_t = 0$ in Equation (1). Then, the process output e_t follows:

$$e_t = X_{t-1} + D_t \tag{3}$$

The one-step-ahead forecast error of the process disturbance D_t that minimises the MSE is $e_t(1) = D_{t+1} - \widehat{D}_t(1) = a_{t+1}$ given by Box, Jenkins, and Reinsel (2013) on the condition that D_t follows an AR(p) model. Then, the one-step-ahead forecast equation of D_t for an AR(p) model is

$$\widehat{D}_t(1) = D_{t+1} - a_{t+1} = (\varphi_1 + \varphi_2 B + \cdots + \varphi_p B^{p-1})D_t = \frac{\varphi_1 + \varphi_2 B + \cdots + \varphi_p B^{p-1}}{1 - \varphi_1 B - \cdots - \varphi_p B^p} a_t \tag{4}$$

In order to ensure that e_{t+1} does not deviate from its target value of zero, the manipulated variable X_t, based on Equation (3), should satisfy $X_t = -\widehat{D}_t(1)$, i.e.:

$$X_t = -\frac{\varphi_1 + \varphi_2 B + \cdots + \varphi_p B^{p-1}}{1 - \varphi_1 B - \cdots - \varphi_p B^p} a_t \tag{5}$$

Now substituting Equations (2) and (5) into Equation (3), then e_t becomes:

$$e_t = -\frac{\varphi_1 + \varphi_2 B + \cdots + \varphi_p B^{p-1}}{1 - \varphi_1 B - \cdots - \varphi_p B^p} a_{t-1} + \frac{1}{1 - \varphi_1 B - \cdots - \varphi_p B^p} a_t$$

$$\Rightarrow (1 - \varphi_1 B - \cdots - \varphi_p B^p)e_t = -(\varphi_1 + \varphi_2 B + \cdots + \varphi_p B^{p-1})a_{t-1} + a_t = (1 - \varphi_1 B - \cdots - \varphi_p B^p)a_t$$

that is,

$$e_t = a_t \tag{6}$$

By Equation (6), MMSE-controlled process outputs are adjusted to a white noise series and eliminate its auto-correlated characteristic, and $\sigma_e^2 = \sigma_a^2$. Substituting Equation (6) into Equation (5), under the AR(p) disturbance process, the MMSE controller can be obtained:

$$X_t = -\frac{\varphi_1 + \varphi_2 B + \cdots + \varphi_p B^{p-1}}{1 - \varphi_1 B - \cdots - \varphi_p B^p} e_t \tag{7}$$

and Equation (7) becomes

$$X_t - \varphi_1 X_{t-1} - \cdots - \varphi_p X_{t-p} = -\varphi_1 \left(e_t + \frac{\varphi_2}{\varphi_1} e_{t-1} + \cdots + \frac{\varphi_p}{\varphi_1} e_{t-p+1} \right) \tag{8}$$

Since the ARMA process of Equation (8) is stationary, the manipulated variable X_t can be expanded into $X_t = -\varphi_1 \sum_{k=0}^{\infty} G_k e_{t-k}$, where G_k is Green function and the variance of X_t follows:

$$\sigma_X^2 = \varphi_1^2 \sigma_e^2 \sum_{k=0}^{\infty} G_k^2 \tag{9}$$

Assume that there are no identical roots in the characteristic equation of Equation (8) and that $\lambda_1, \lambda_2, \ldots, \lambda_p$ are p different roots, which can be determined by solving the equation $\lambda^p - \varphi_1 \lambda^{p-1} - \cdots - \varphi_p = 0$. Then, Green function G_k can be written as:

$$G_k = g_1 \lambda_1^k + g_2 \lambda_2^k + \cdots + g_p \lambda_p^k \tag{10}$$

where

$$g_i = \frac{\lambda_i^{p-1} + \frac{\varphi_2}{\varphi_1} \lambda_i^{p-2} + \cdots + \frac{\varphi_p}{\varphi_1}}{\prod_{\substack{j=1 \\ j \neq i}}^{p} (\lambda_i - \lambda_j)} = \frac{1}{\varphi_1} \frac{\varphi_1 \lambda_i^{p-1} + \varphi_2 \lambda_i^{p-2} + \cdots + \varphi_p}{\prod_{\substack{j=1 \\ j \neq i}}^{p} (\lambda_i - \lambda_j)} = \frac{1}{\varphi_1} \frac{\lambda_i^p}{\prod_{\substack{j=1 \\ j \neq i}}^{p} (\lambda_i - \lambda_j)} \tag{11}$$

Substituting Equation (11) into Equation (10), then G_k becomes:

$$G_k = \frac{1}{\varphi_1} \sum_{i=1}^{p} \frac{\lambda_i^{p+k}}{\prod_{\substack{j=1 \\ j \neq i}}^{p} (\lambda_i - \lambda_j)} \tag{12}$$

Substituting Equation (12) into Equation (9), then the variance of X_t is

$$\sigma_X^2 = \sigma_e^2 \sum_{k=0}^{\infty} \left[\sum_{i=1}^{p} \frac{\lambda_i^{p+k}}{\prod_{\substack{j=1 \\ j \neq i}}^{p} (\lambda_i - \lambda_j)} \right]^2 \tag{13}$$

where $\lambda_1, \lambda_2, \ldots, \lambda_p$ are the roots of the characteristic equation $\lambda^p - \varphi_1\lambda^{p-1} - \cdots - \varphi_p = 0$, and Equation (13) is convergent because $|\lambda_i| < 1$.

When the disturbance model of the process is AR(2) model, the solution of Equation (13) has the form:

$$\sigma_X^2 = \frac{\sigma_e^2}{(\lambda_1 - \lambda_2)^2}\left(\frac{\lambda_1^4}{1-\lambda_1^2} + \frac{\lambda_2^4}{1-\lambda_2^2} - \frac{2\lambda_1^2\lambda_2^2}{1-\lambda_1\lambda_2}\right) \tag{14}$$

where λ_1 and λ_2 are two different roots of the equation $\lambda^2 - \varphi_1\lambda - \varphi_2 = 0$.

3. SPC monitoring of MMSE-controlled outputs

3.1 *The expectation of process outputs*

Now suppose a step shift of $\delta\sigma_e$ occurs in the process after instant $t = 0$ (Wardell, Moskowitz, and Plante 1994), i.e.:

$$\mu_t = \begin{cases} 0, & t \le 0 \\ \delta\sigma_e, & t > 0 \end{cases} \tag{15}$$

Substituting Equations (2), (7) and (15) into Equation (1), the process output can be obtained as:

$$e_t = -\frac{\varphi_1 + \varphi_2 B + \cdots + \varphi_p B^{p-1}}{1 - \varphi_1 B - \cdots - \varphi_p B^p} e_{t-1} + \frac{1}{1 - \varphi_1 B - \cdots - \varphi_p B^p} a_t + \mu_t, t \ge 1$$

$$\Rightarrow (1 - \varphi_1 B - \cdots - \varphi_p B^p) e_t = -(\varphi_1 + \varphi_2 B + \cdots + \varphi_p B^{p-1}) e_{t-1} + a_t + (1 - \varphi_1 B - \cdots - \varphi_p B^p)\mu_t$$

i.e.

$$e_t = a_t + (1 - \varphi_1 B - \cdots - \varphi_p B^p)\mu_t, t \ge 1 \tag{16}$$

Then, the mathematical expectation of e_t is

$$E(e_t) = \begin{cases} \mu, & t = 1 \\ \left(1 - \sum_{i=1}^{t-1} \varphi_i\right)\mu, & 2 \le t \le p+1 \\ \left(1 - \sum_{i=1}^{p} \varphi_i\right)\mu, & t > p+1 \end{cases} \tag{17}$$

Similarly, the mathematical expectation of X_{t-1} is

$$E(X_{t-1}) = \begin{cases} 0, & t = 1 \\ -\left(\sum_{i=1}^{t-1} \varphi_i\right)\mu, & 2 \le t \le p+1 \\ -\left(\sum_{i=1}^{p} \varphi_i\right)\mu, & t > p+1 \end{cases} \tag{18}$$

3.2 *The ARL of the output chart*

The evaluation index ARL is used to assess the performance of the SPC monitoring. The traditional Shewhart chart can be used to monitor the process output e_t, which meets the IID characteristic. Let L_e denote the coefficient of the control limits of the output chart, and p_t denote the probability that e_t locates within control limits at instant t, then:

$$\begin{aligned} p_t = \Phi\{-L_e\sigma_e < e_t < L_e\sigma_e\} &= \Phi\left\{\tfrac{-L_e\sigma_e - E(e_t)}{\sigma_e} < U < \tfrac{L_e\sigma_e - E(e_t)}{\sigma_e}\right\} \\ &= \Phi\left\{-L_e - \tfrac{E(e_t)}{\sigma_e} < U < L_e - \tfrac{E(e_t)}{\sigma_e}\right\} \end{aligned}$$

Namely

$$p_t = \begin{cases} \Phi(L_e-\delta)-\Phi(-L_e-\delta), & t=1 \\ \Phi\left\{L_e-\left(1-\sum_{i=1}^{t-1}\varphi_i\right)\delta\right\}-\Phi\left\{-L_e-\left(1-\sum_{i=1}^{t-1}\varphi_i\right)\delta\right\}, & 2\le t\le p+1 \\ \Phi\left\{L_e-\left(1-\sum_{i=1}^{p}\varphi_i\right)\delta\right\}-\Phi\left\{-L_e-\left(1-\sum_{i=1}^{p}\varphi_i\right)\delta\right\}, & t>p+1 \end{cases} \tag{19}$$

Let $\Pr(t)$ denote the probability that the Shewhart chart gives an out-of-control signal at instant t, then $\Pr(t)$ is given by:

$$\Pr(t) = \begin{cases} 1-p_1, & t=1 \\ (1-p_t)\prod_{i=1}^{t-1}p_i, & 2\le t\le p+1 \\ p_{p+1}^{t-p-1}(1-p_{p+1})\prod_{i=1}^{p}p_i, & t>p+1 \end{cases} \tag{20}$$

When $p = 1$,

$$\Pr(t) = \begin{cases} 1-p_1, & t=1 \\ p_1p_2^{t-2}(1-p_2), & t\ge 2 \end{cases}$$

Then,

$$\mathrm{ARL}^e = \sum_{k=1}^{\infty} k\Pr(k) = 1-p_1+\sum_{k=2}^{\infty} kp_1p_2^{k-2}(1-p_2) = 1-p_1+p_1(1-p_2)\frac{1}{p_2}\left(\sum_{k=1}^{\infty} kp_2^{k-1}-1\right)$$

$$\mathrm{ARL}^e = \frac{1+p_1-p_2}{1-p_2}$$

where $\sum_{k=1}^{\infty} kx^{k-1} = \frac{1}{(1-x)^2},\ |x|<1$.

That is, $\mathrm{ARL}^e = \frac{1+p_1-p_2}{1-p_2}$.

When $p \ge 2$,

$$\mathrm{ARL}^e = 1\cdot\Pr(1)+\cdots+p\cdot\Pr(p)+\sum_{k=p+1}^{\infty} k\Pr(k)$$

$$\mathrm{ARL}^e = 1\cdot(1-p_1)+\cdots+p\cdot p_1\cdots p_{p-1}(1-p_p)+\sum_{k=p+1}^{\infty} kp_1\ldots p_p(1-p_{p+1})p_{p+1}^{k-p-1}$$

$$\mathrm{ARL}^e = 1-p_1+\sum_{i=2}^{p} i(1-p_i)\prod_{j=1}^{i-1}p_j+p_1\cdots p_p(1-p_{p+1})\sum_{k=p+1}^{\infty} kp_{p+1}^{k-p-1}$$

and

$$\sum_{k=p}^{\infty} kp_p^{k-p} = \sum_{k=0}^{\infty}(k+p+1)p_{p+1}^k = p_{p+1}\left(\sum_{k=1}^{\infty} kp_{p+1}^{k-1}\right)+(p+1)\sum_{k=0}^{\infty}p_{p+1}^k = \frac{p_{p+1}}{(1-p_{p+1})^2}+\frac{p+1}{1-p_{p+1}}$$

$$\mathrm{ARL}^e = 1-p_1+\sum_{i=2}^{p} i(1-p_i)\prod_{j=1}^{i-1}p_j+p_1\cdots p_p(1-p_{p+1})\left[\frac{p_{p+1}}{(1-p_{p+1})^2}+\frac{p+1}{1-p_{p+1}}\right]$$

$$\mathrm{ARL}^e = 1-p_1+\sum_{i=2}^{p} i(1-p_i)\prod_{j=1}^{i-1}p_j+\left(\frac{p_{p+1}}{1-p_{p+1}}+p+1\right)\prod_{i=1}^{p}p_i$$

Therefore,

$$\mathrm{ARL}^e = \begin{cases} \frac{1+p_1-p_2}{1-p_2}, & p=1 \\ 1-p_1+\sum_{i=2}^{p} i(1-p_i)\prod_{j=1}^{i-1} p_j + \left(\frac{p_{p+1}}{1-p_{p+1}}+p+1\right)\prod_{k=1}^{p} p_k, & p\geq 2 \end{cases} \tag{21}$$

where p_i, p_j, p_k can be obtained by solving Equation (19). In particular, when $p = 2$, the solution of Equation (21) has the form:

$$\mathrm{ARL}^e = 1 + p_1 + \frac{p_1 p_2}{1-p_3} \tag{22}$$

Because X_t is the linear combination of the sets of $\{e_t\}$, which can be seen from Equation (7), X_t follows the normal distribution. Let L_X denote the coefficient of the control limits of the input Shewhart chart. Similarly, the probability that X_{t-1} locates within control limits can be obtained as:

$$p'_t = \begin{cases} \Phi(L_X) - \Phi(-L_X), & t=1 \\ \Phi\left\{L_X + \frac{\sigma_e}{\sigma_X}\left(\sum_{i=1}^{t-1}\varphi_i\right)\delta\right\} - \Phi\left\{-L_X + \frac{\sigma_e}{\sigma_X}\left(\sum_{i=1}^{t-1}\varphi_i\right)\delta\right\}, & 2\leq t\leq p+1 \\ \Phi\left\{L_X + \frac{\sigma_e}{\sigma_X}\left(\sum_{i=1}^{p}\varphi_i\right)\delta\right\} - \Phi\left\{-L_X + \frac{\sigma_e}{\sigma_X}\left(\sum_{i=1}^{p}\varphi_i\right)\delta\right\}, & t>p+1 \end{cases} \tag{23}$$

Then, the ARLs of the input Shewhart chart can be obtained by Equation (21), if only p_t in Equation (21) is replaced by p'_t.

4. The proposed joint monitoring chart

4.1 *Design of the joint monitoring chart*

In an attempt to simultaneously monitor the manipulated variable and the process output, the bivariate random variable (X, Z) is chosen to be the monitored characteristics, where $X = \left\{\frac{X_{t-1}}{\sigma_X}\right\}$ and $Z = \left\{\frac{e_t}{\sigma_e}\right\}$. X and Z are uncorrelated because $\mathrm{cov}(X_{t-1}, e_t) = 0$, which can be seen from Equation (7). Let $f(x, z)$ denote the joint probability density function of (X, Z), and α denote the overall false alarm probability. In view of the fact that the overall process variability can be illustrated by the distance from the plotted point to the origin of coordinates, the joint chart can monitor the circular areas, whose radius L follows:

$$\iint_{x^2+z^2\leq L^2} f(x,z)\mathrm{d}x\mathrm{d}z = 1-\alpha \tag{24}$$

The radius of the monitoring areas of the joint chart is chosen to achieve a specific in-control ARL_0, which is determined via Monte Carlo simulation.

(1) The first out-of-control rule

The joint chart gives an out-of-control signal as soon as a monitoring point exceeds the in-control areas in Figure 1. That is:

$$\sqrt{\left(\frac{X_{t-1}}{\sigma_X}\right)^2 + \left(\frac{e_t}{\sigma_e}\right)^2} \geq L \tag{25}$$

(2) The second out-of-control rule

If the plotted points falling within the control limits exhibit a certain non-random pattern of behaviour, the process is also out of control. Because X_{t-1} is auto-correlated in the bivariate random variable (X, Z), the auto-correlations of manipulated variables make it difficult to obtain the probability that non-random events occur in the joint chart.

The event A that m sequential points locate within the control limits but locate in the same quadrant is an exception. Take the first quadrant as an example, the occurrence probability of the event A follows $P(A)\leq P\{z_1, z_2, \ldots, z_m \in (0, L)\} = [P\{Z\in(0,L)\}]^m$, where $P\{Z\in(0,L)\} = \Phi(L) - 0.5$ and $\alpha = P(A)\leq(\Phi(L)-0.5)^m$, then m can be obtained as:

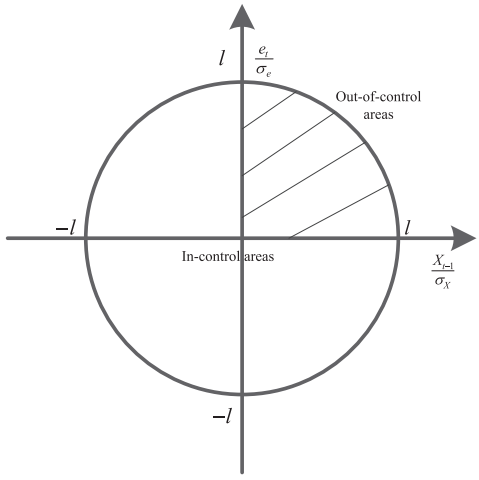

Figure 1. The monitoring areas of the joint chart.

$$m = \left[\frac{\log \alpha}{\log(\Phi(L) - 0.5)}\right] \tag{26}$$

where the symbol [ ] denotes the integral function.

For example, assume that the bivariate random variable (X, Z) follows the bivariate normal distribution, that is $f(x,z) = \frac{1}{2\pi}\exp\{-\frac{x^2+z^2}{2}\}$, and let $\alpha = 0.0027$, then $m = 8$ by solving Equations (25) and (26). In other words, the joint chart will give an out-of-control signal when eight sequential plotted points locate in the same quadrant.

4.2 *Performance analysis of the joint monitoring chart*

The ARL property is investigated to evaluate the performance of the joint chart in this section. Because ARMA(1, 1) model includes AR(1) model, the simulation analysis for AR(1) models is no longer needed at here. Then, judging from Equation (21), when $p \geq 2$, the ARLs of the output chart and the input chart are the functions with respect to p_1, p_2, … ,p_p, respectively, and p_i is the function with respect to $\sum_{i=1}^{p} \varphi_i$ judging from Equation (23), namely the variation law of the ARLs mainly depends on $\sum_{i=1}^{p} \varphi_i$. On behalf of all high-order AR(p) model, the AR(2) model is hereby applied to conduct the performance analysis.

In order to fairly compare the performance of the output chart, the input chart and the joint chart, their coefficients of the control limits are adjusted so that the in-control ARL_0 equals 370. Then, under different mean shifts including $\delta = 0.5$, 1, 3 and 5, Tables 1 and 2 present the ARLs of the output chart, the input chart and the joint chart of ten MMSE-controlled stationary AR(2) processes when the parameter $\varphi_1 < 0$ and $\varphi_1 > 0$, respectively. The ARLs of the output chart and the input chart can be obtained by solving Equation (22), while the ARLs of the joint chart only can be obtained by means of Monte Carlo simulation.

The ARLs in Tables 1 and 2 show that the joint chart can take advantage of strengths of the output chart and the input chart under various AR(2) processes to improve the monitoring performance. The major findings are

(1) For large mean shifts ($\delta \geq 5$), monitoring the process output is always more efficient than monitoring the manipulated action. For small mean shifts ($\delta \leq 3$), the better choice depends on the values of φ_1. When $\varphi_1 < 0$, monitoring the process output is more efficient; when $\varphi_1 > 0$, exactly the opposite.

    In terms of small mean shifts, a further detailed analysis is implemented. Figures 2 and 3 are the contour plots of the ARLs for the output chart when $\varphi_1 < 0$ and the input chart $\varphi_1 > 0$, respectively. We can draw a conclusion that the output chart, compared to the input chart in Table 1, has an excellent monitoring performance when $\varphi_1 < 0$ by the fact that most of ARLs are lower than 50 in Figure 2. However, only few of ARLs of the input chart are lower than 50 in Figure 3. It demonstrates that the input chart is still not a good choice in terms of monitoring performance.

(2) When the values of $\varphi_1 + \varphi_2$ are closer to 1, the monitoring performances of the output chart, the input chart and the joint chart will be worse. As is illustrated in Equation (19), the monitoring performances of the output chart,

Table 1. ARL comparisons of output, input and joint charts ($\varphi_1 < 0$).

		ARL			
(φ_1, φ_2)	δ	Output	Input	Joint	Tsung's
(–1.5, −0.56)				$L = 3.316$	$L = 3.206$
	0	370.40	370.40	369.89	735.66
	0.5	15.47	292.25	21.29	22.80
	1	3.27	157.31	3.81	3.87
	3	1.50	16.66	1.63	1.59
	5	1.02	5.23	1.05	1.04
(–1.1, –0.30)				$L = 3.335$	$L = 3.206$
	0	370.40	370.40	369.16	743.01
	0.5	28.93	196.83	35.96	45.78
	1	4.88	68.55	5.69	6.08
	3	1.50	4.99	1.63	1.58
	5	1.02	2.43	1.05	1.04
(–1.0, −0.10)				$L = 3.314$	$L = 3.206$
	0	370.40	370.40	369.46	741.18
	0.5	39.90	279.07	51.59	63.93
	1	6.44	153.66	8.39	8.50
	3	1.50	14.59	1.63	1.58
	5	1.02	4.05	1.05	1.04
(–0.9, −0.08)				$L = 3.328$	$L = 3.206$
	0	370.40	370.40	369.57	736.13
	0.5	45.75	237.46	57.23	75.36
	1	7.47	108.09	9.27	10.14
	3	1.50	8.18	1.63	1.58
	5	1.02	2.82	1.05	1.04
(–0.6, 0.16)				$L = 3.328$	$L = 3.206$
	0	370.40	370.40	370.71	730.38
	0.5	87.90	302.41	106.95	154.39
	1	17.10	185.87	22.27	26.28
	3	1.52	22.38	1.66	1.62
	5	1.02	4.82	1.05	1.04
(–0.5, 0.14)				$L = 3.336$	$L = 3.206$
	0	370.40	370.40	369.27	738.90
	0.5	97.39	281.07	115.15	171.91
	1	20.03	160.04	25.19	30.75
	3	1.54	15.85	1.67	1.65
	5	1.02	3.24	1.05	1.04
(–0.5, −0.06)				$L = 3.341$	$L = 3.206$
	0	370.40	370.40	370.59	737.24
	0.5	75.85	148.84	77.64	131.37
	1	14.15	41.53	13.45	20.88
	3	1.54	3.06	1.65	1.64
	5	1.02	2.05	1.05	1.04
(–0.1, 0.56)				$L = 3.341$	$L = 3.206$
	0	370.40	370.40	370.06	738.29
	0.5	268.23	247.41	261.01	513.83
	1	134.78	113.99	121.07	247.77
	3	3.78	10.17	4.19	6.39
	5	1.02	3.86	1.05	1.04
(–0.1, 0.30)				$L = 3.361$	$L = 3.206$
	0	370.40	370.40	369.83	738.38
	0.5	199.32	261.79	216.04	373.88
	1	69.89	129.81	78.82	122.28
	3	2.19	11.58	2.75	2.87
	5	1.02	4.09	1.05	1.04

(*Continued*)

Table 1. (*Continued*).

(φ_1, φ_2)	δ	ARL			
		Output	Input	Joint	Tsung's
(–0.1, 0.06)				$L = 3.357$	$L = 3.206$
	0	370.40	370.40	369.88	738.35
	0.5	147.36	327.21	175.20	269.27
	1	39.91	241.10	53.15	66.34
	3	1.85	35.46	2.01	2.16
	5	1.02	3.64	1.05	1.04

the input chart and the joint chart sharply decline when $\varphi_1 + \varphi_2 \rightarrow 1$. For example, when $\varphi_1 = 1.1$ and $\varphi_2 = -0.24$ or $\varphi_1 = 1.6$ and $\varphi_2 = -0.64$ in Table 2, those charts are not very efficient.

(3) For large mean shifts ($\delta \geq 5$), the monitoring performance of the joint chart is generally similar to that of the better one in the individual chart. For small mean shifts ($\delta \leq 3$), when $\varphi_1 < 0$, the ARLs of the joint chart are in close proximity to those of the output chart with better monitoring performance; when $\varphi_1 > 0$, the joint chart is similar to the individual output chart and it is significantly superior to the individual input chart.

(4) Our joint chart outperforms the joint chart based on Bonferroni's approach developed by Tsung, Shi, and Wu (1999) in most of the cases, but slightly worsens for large mean shifts ($\delta \geq 5$) when $\varphi_1 < 0$. Particularly when smaller mean shifts ($\delta \leq 3$) occur, our joint chart has an overwhelming predominance than the joint chart based on Bonferroni's approach developed by Tsung, Shi, and Wu (1999).

Furthermore, a specific analysis is taken for the joint chart under small mean shifts. Figures 4 and 5 are the contour plots of the ARLs for the joint chart when $\delta = 1$ and $\delta = 3$, respectively. These two figures show that most of ARLs are lower than 100 when $\delta = 1$ and that most of ARLs are lower than 50 when $\delta = 3$. From Figures 4 and 5, the conclusion can be drawn that the joint chart can perform well under most of the processes. Regardless of small mean shifts or large mean shifts, the joint chart shows a significant improvement over the individual chart, including the output chart and the input chart. In particular, whether or not monitoring the process output or the control action, the joint chart will be always a good choice for a complicated disturbance process.

5. Case studies

5.1 *Case study I*

As revealed in Figure 6, an example with real data from the manufacturing process of the inner diameter $\Phi 22_0^{0.03}$ of a valve shell is used to illustrate the proposed joint monitoring chart. The machining process is implemented using a computer numerical control (CNC) machining centre (CTX420). Figure 7 shows the machining process of the valve shell.

The GARCH toolbox of MATLAB is adopted to model the AR(p) process of the real cases. The model construction method is described as follows. Firstly, the 'garchset' function, based on the model selection criteria, namely Akaike information criterion (Shumway and Stoffer 2010, 213) is used to fit the best and the order p. Secondly, the 'garchfit' function, based on maximum likelihood estimate, is used to accurately estimate the parameters of the AR(p) model. This model construction method is also applied to the rest of case studies.

After a long-time data collection and fitting their time series model, an AR(6) model is appropriate, which can be written as:

$$D_t = 0.0475D_{t-1} - 0.0178D_{t-2} + 0.0714D_{t-3} - 0.0528D_{t-4} - 0.0141D_{t-5} + 0.0619D_{t-6} + a_t \tag{27}$$

where $\hat{\sigma}_a^2 = 3.47^2$ and $\hat{\sigma}_D^2 = 3.51^2$.

By means of an investigation of the machining centre, a manipulated variable X_t (the cutting speed of CNC) is available for adjusting the process and X_t immediately has its full effect on Y_{t+1}. To reduce the process variability, the MMSE controller can be designed as:

$$\begin{aligned} X_t = {} & 0.0475X_{t-1} - 0.0178X_{t-2} + 0.0714X_{t-3} - 0.0528X_{t-4} - 0.0141X_{t-5} + 0.0619X_{t-6} - 0.0475e_t + 0.0178e_{t-1} \\ & - 0.0714e_{t-2} + 0.0528e_{t-3} + 0.0141e_{t-4} - 0.0619e_{t-5} \end{aligned} \tag{28}$$

where $\hat{\sigma}_X^2 = 0.42^2$.

Table 2. ARL comparisons of output, input and joint charts ($\varphi_1 > 0$).

		ARL			
(φ_1, φ_2)	δ	Output	Input	Joint	Tsung's
(0.1, 0.06)				$L = 3.358$	$L = 3.206$
	0	370.40	370.40	370.65	729.46
	0.5	190.06	104.96	140.09	211.13
	1	64.10	25.05	33.53	43.75
	3	2.48	2.89	2.07	2.26
	5	1.02	2.15	1.05	1.04
(0.1, 0.30)				$L = 3.359$	$L = 3.206$
	0	370.40	370.40	370.16	730.95
	0.5	252.08	129.14	175.61	265.28
	1	116.82	32.49	53.17	66.14
	3	4.18	3.47	2.64	3.09
	5	1.03	2.94	1.06	1.04
(0.1, 0.56)				$L = 3.343$	$L = 3.206$
	0	370.40	370.40	369.73	733.65
	0.5	321.75	174.64	248.86	416.95
	1	223.83	58.78	110.99	140.40
	3	14.44	4.58	5.31	7.09
	5	1.04	3.05	1.07	1.09
(0.4, −0.04)				$L = 3.341$	$L = 3.206$
	0	370.40	370.40	369.25	739.36
	0.5	241.54	183.70	209.30	354.38
	1	106.47	62.13	73.21	109.35
	3	4.66	3.58	3.09	4.01
	5	1.04	2.05	1.06	1.07
(0.6, 0.16)				$L = 3.331$	$L = 3.206$
	0	370.40	370.40	369.11	736.76
	0.5	344.36	217.24	295.04	648.49
	1	280.77	89.29	172.54	277.26
	3	43.77	6.36	13.21	19.09
	5	1.56	2.85	1.25	2.47
(0.7, 0.08)				$L = 3.330$	$L = 3.206$
	0	370.40	370.40	369.06	741.27
	0.5	348.15	232.75	302.81	678.94
	1	291.76	98.79	191.26	317.46
	3	51.77	7.74	16.89	25.12
	5	1.76	2.65	1.33	3.01
(0.9, −0.20)				$L = 3.339$	$L = 3.206$
	0	370.40	370.40	369.05	744.44
	0.5	332.02	254.35	300.04	568.46
	1	248.65	121.38	181.59	268.36
	3	29.30	8.37	13.68	19.73
	5	1.36	2.42	1.27	1.91
(1.0, −0.16)				$L = 3.330$	$L = 3.206$
	0	370.40	370.40	369.86	735.99
	0.5	357.76	287.25	330.87	705.91
	1	322.09	159.07	253.02	490.84
	3	82.99	17.03	35.20	61.15
	5	2.65	4.17	1.82	5.76
(1.1, −0.24)				$L = 3.330$	$L = 3.206$
	0	370.40	370.40	370.63	741.37
	0.5	360.33	299.16	340.82	724.34
	1	330.86	186.39	272.04	586.31
	3	96.31	21.27	45.04	86.36
	5	3.11	5.60	2.14	6.78
(1.6, −0.64)				$L = 3.310$	$L = 3.206$
	0	370.40	370.40	370.71	742.07
	0.5	367.83	358.63	366.57	731.20

(*Continued*)

Table 2. (*Continued*).

(φ_1, φ_2)	δ	ARL			
		Output	Input	Joint	Tsung's
	1	358.10	323.44	352.34	716.14
	3	154.46	162.15	157.39	366.78
	5	4.53	73.58	5.68	14.75

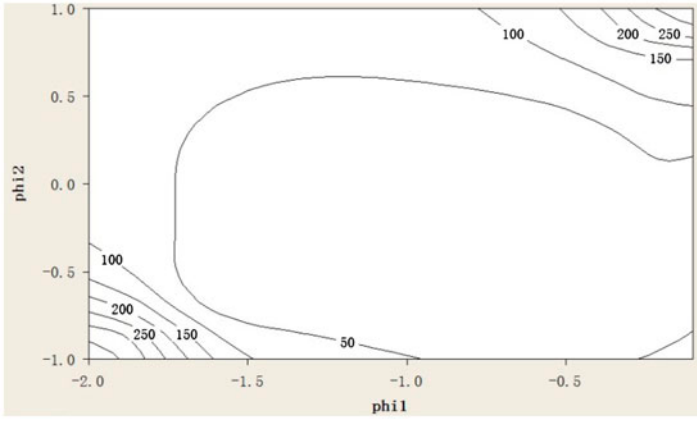

Figure 2. ARL of the output chart when $\delta = 1$ (phi1 < 0).

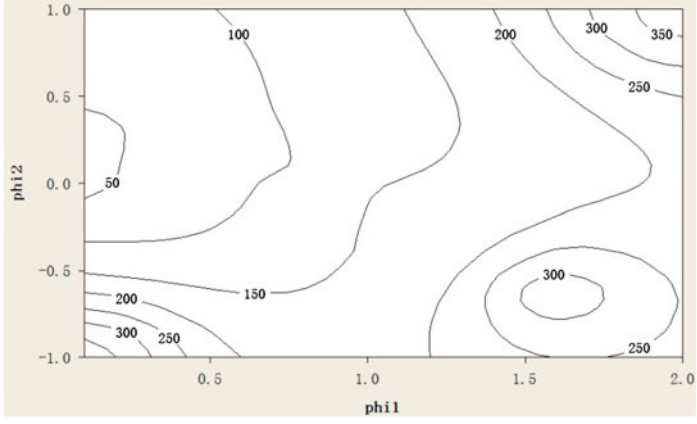

Figure 3. ARL of the input chart when $\delta = 1$ (phi1 > 0).

To illustrate the monitoring performance, 30 observations for a bulk-production, under a normal in-control process, are chosen to artificially add a mean shift of $\mu = 2 \cdot \sigma_e$ at instant $t = 0$ as a special cause of the process by manipulated variables. For better revealing differences between our joint chart and the joint chart based on Bonferroni's approach developed by Tsung, Shi, and Wu (1999), the two joint charts are compared with each other. Figures 7 and 8 show their monitoring information, respectively. Because $\alpha = 0.27\%$, the in-control radius L is 3.405 in our joint chart in Figure 8, and the coefficient of the control limits $L_e = L_X = Z_{(1-\alpha/4)} = 3.206$ using Bonferroni's approach in Figure 9.

According to the developed first and second out-of-control rules, Figure 8 shows that there are no sequential eight plotted points from observation 1 to 30, which locate in the same quadrant, and that our joint chart signals the $\mu = 2 \cdot \sigma_e$ mean shift at observation 21. Figure 9 shows that joint chart by Tsung, Shi, and Wu (1999) also signals at observation 21. The monitoring information indicates that our joint chart is comparable with Tsung, Shi, and Wu's (1999) joint

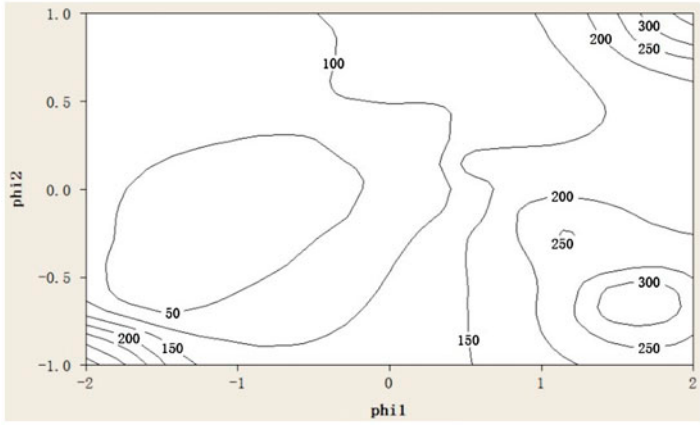

Figure 4. ARL of the joint chart when $\delta = 1$.

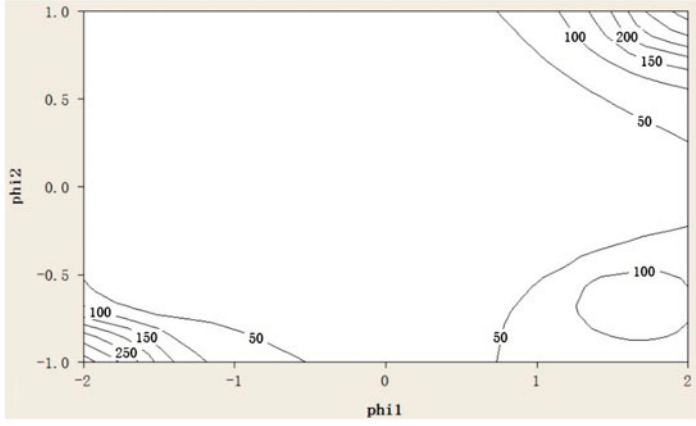

Figure 5. ARL of the joint chart when $\delta = 3$.

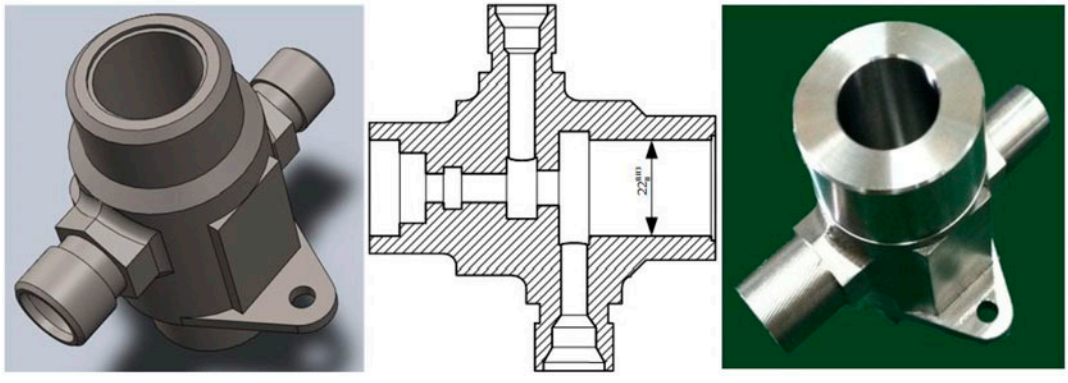

Figure 6. A valve shell.

chart and that our joint chart can efficiently signal the out-of-control information. At last, it is important to note that since the MMSE controller needs to compensate for the mean shift, there are some adjustments to manipulated inputs in both joint charts.

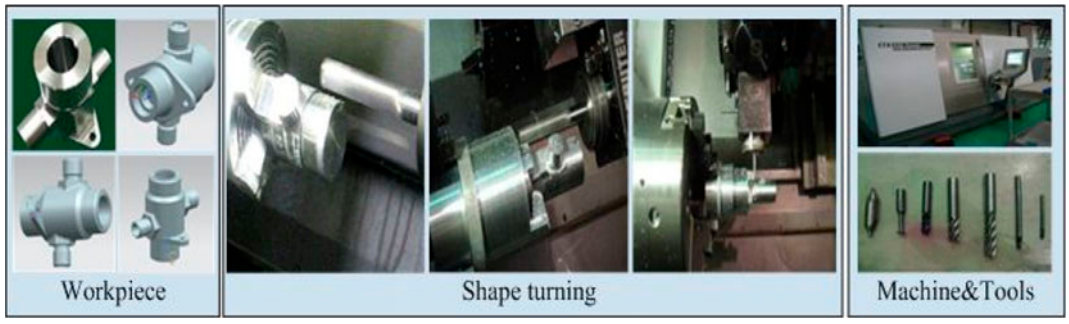

Figure 7. Workpiece machining process.

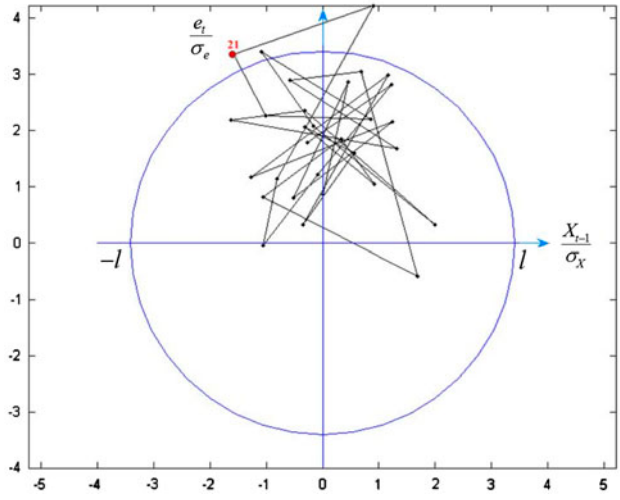

Figure 8. Our joint chart under an AR(6) process.

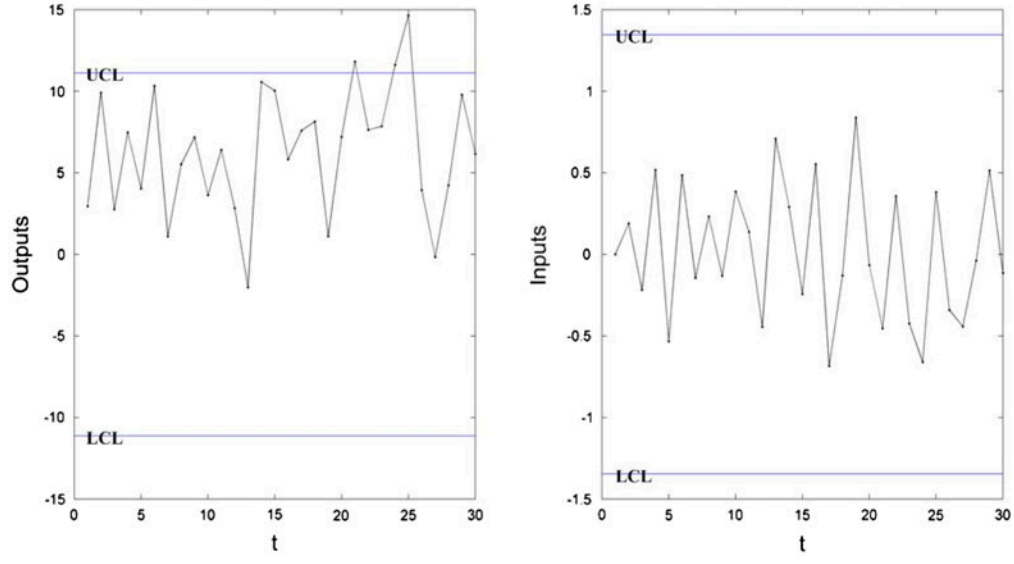

Figure 9. Tsung, Shi, and Wu's (1999) joint chart under an AR(6) process.

5.2 *Case study II*

The second example is a production processing of a tension spring in a steel wire ringer. An AR(5) disturbance model is adequate for its quality characteristic in terms of tensile stress, that is:

$$D_t = 0.2977D_{t-1} + 0.0056D_{t-2} + 0.2969D_{t-3} - 0.2286D_{t-4} + 0.1717D_{t-5} + a_t \tag{29}$$

where $\hat{\sigma}_a^2 = 1.21^2$ and $\hat{\sigma}_D^2 = 1.37^2$.

Similarly, detailed procedures are consistent with the first example. Figures 10 and 11 show the monitoring information of our joint chart and Tsung, Shi, and Wu's (1999) joint chart, respectively. The two charts all signal the mean shift at observations 3, which again demonstrates that our joint chart is not inferior to Tsung, Shi, and Wu's (1999) joint chart.

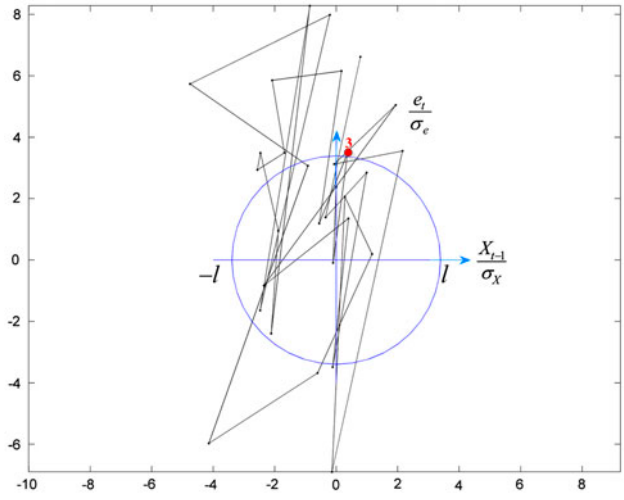

Figure 10. Our joint chart under an AR(5) process.

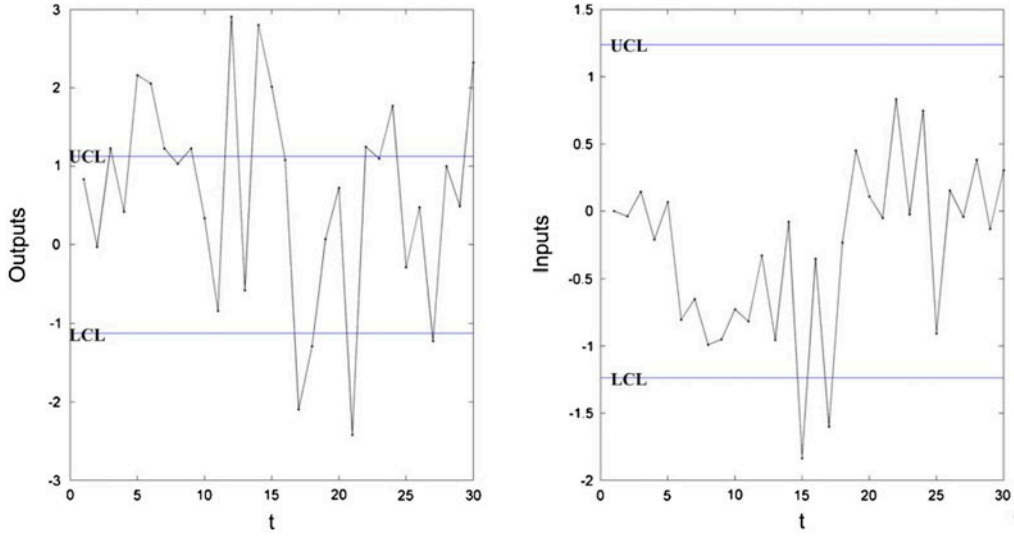

Figure 11. Tsung, Shi, and Wu's (1999) joint chart under an AR(5) process.

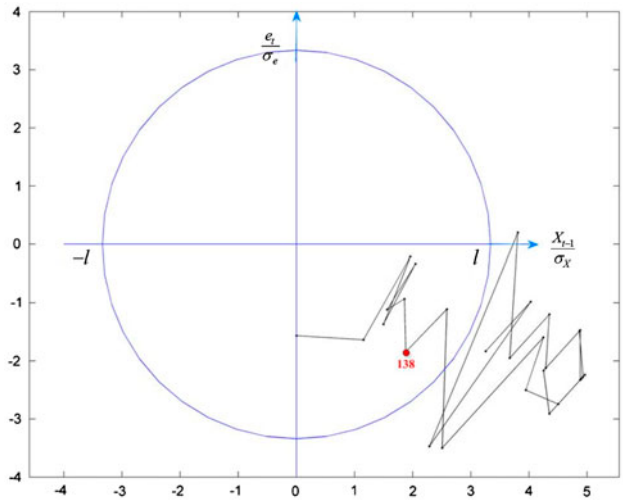

Figure 12. Our joint chart under an AR(4) process.

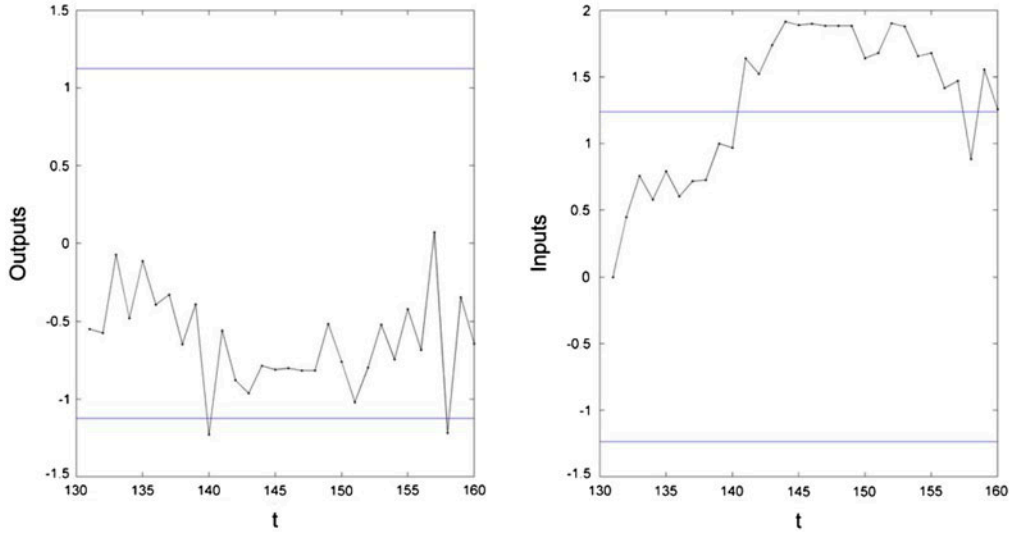

Figure 13. Tsung, Shi, and Wu's (1999) joint chart under an AR(4) process.

5.3 *Case study III*

The last example is taken from Pandit and Wu's (1983, 398) textbook, which lists 160 observations of a gate-opening regulation in a paper-making process. The first 100 normal observations are used to fit its time series model. The last 30 observations, having a small mean shift, are used to test the joint chart. The following AR(4) model is appropriate for this data:

$$D_t = 0.8106D_{t-1} - 0.1289D_{t-2} + 0.0664D_{t-3} - 0.0504D_{t-4} + a_t \tag{30}$$

where $\hat{\sigma}_a^2 = 0.351^2$ and $\hat{\sigma}_D^2 = 0.522^2$.

Assume a control action X_t can be found out to adjust the gate opening in the paper-making process. Then, the MMSE controller can be designed as:

$$X_t = 0.8106X_{t-1} - 0.1289X_{t-2} + 0.0664X_{t-3} - 0.0504X_{t-4} - 0.8106e_t + 0.1289e_{t-1} - 0.0664e_{t-2} + 0.0504e_{t-3} \tag{31}$$

where $\hat{\sigma}_X^2 = 0.386^2$.

Under the condition that $\alpha = 0.27\%$ the in-control radius L is 3.339 and our joint chart is shown in Figure 12. Our joint chart signals a mean shift at observation 138, because eight sequential plotted points locate in the fourth quadrant. However, Tsung, Shi, and Wu's (1999) joint chart does not give an out-of-control signal until observation 140 in Figure 13. Our joint chart has been shown to possess better monitoring performances than Tsung, Shi, and Wu's (1999) joint chart in monitoring smaller mean shifts in this case.

6. Conclusions

A new joint monitoring scheme is presented for processes with arbitrary order AR(p) disturbance to simultaneously monitor the control action and the process output. The ARLs of the proposed joint chart, which can be applied to monitor any stationary high-order disturbance process, have been compared with the individual input and output chart, and Tsung, Shi, and Wu's (1999) joint chart using Bonferroni's approach. Overall, the joint chart can significantly improve the individual monitoring performance. When small mean shifts occur, our joint chart outperforms Tsung, Shi, and Wu's (1999) joint chart for processes with AR(2) disturbance.

It is worth noting that the out-of-control rule that some sequential points are inside the control limits but locate in the same quadrant can improve the monitoring performance of the joint chart to some extent and can be further developed to other non-random pattern of behaviour of those plotted points in future work.

Disclosure statement

No potential conflict of interest was reported by the authors.

Funding

This work was supported by the National Natural Science Foundation of China [grant number 51275558]; National Key Science and Technology Research Program of China [grant number 2014ZX04015-021], and State Key Lab of Mechanical System and Vibration program [grant number MSVZD201503].

References

Bowerman, B. L., and R. T. O'Connell. 1993. *Forecasting and Time Series: An Applied Approach*. Belmont, CA: Duxbury Press.

Box, G. E. P., G. M. Jenkins, and G. C. Reinsel. 2013. *Time Series Analysis: Forecasting and Control*. New York: Wiley.

Box, G. E. P., G. C. Tiao, and S. Bisgaard. 2000. *George Box on Quality and Discovery: Selected Works by GEP Box on Quality, Experimental Design, Control and Robustness*. New York: Wiley.

Brockwell, P. J., and R. A. Davis. 2002. *Introduction to Time Series and Forecasting*. Abingdon: Taylor & Francis.

Du, S., L. Xi, J. Yu, and J. Sun. 2010. "Online Intelligent Monitoring and Diagnosis of Aircraft Horizontal Stabilizer Assemble Processes." *International Journal of Advanced Manufacturing Technology* 50 (1–4): 377–389.

Du, S., and L. Xi. 2011. "Fault Diagnosis in Assembly Processes Based on Engineering-driven Rules and PSOSAEN Algorithm." *Computers & Industrial Engineering* 60 (1): 77–88.

Du, S., L. Xi, J. Ni, E. Pan, and C. R. Liu. 2008. "Product Lifecycle-oriented Quality and Productivity Improvement Based on Stream of Variation Methodology." *Computers in Industry* 59 (2–3): 180–192.

Du, S., Yao, X., and Huang, D. 2015. Engineering Model-based Bayesian Monitoring of Ramp-up Phase of Multistage Manufacturing Process. *International Journal of Production Research* 53(15): 4594–4613.

Jiang, W. 2004. "A Joint Monitoring Scheme for Automatically Controlled Processes." *IIE Transactions* 36 (12): 1201–1210.

Jiang, W., and K. L. Tsui. 2002. "SPC Monitoring of MMSE-and PI-controlled Processes." *Journal of Quality Technology* 34 (4): 384–398.

Messina, W. S., D. C. Montgomery, J. B. Keats, and G. C. Runger. 1996. "Strategies for Statistical Monitoring of Integral Control for the Continuous Process Industries." *Quality and Reliability* 47: 193–214.

Montgomery, D. C. 2009. *Statistical Quality Control*. 6th ed. New York: Wiley.

Montgomery, D. C., J. B. Keats, G. C. Runger, and W. S. Messina. 1994. "Integrating Statistical Process Control and Engineering Process Control." *Journal of Quality Technology* 26 (2): 79–87.

Pandit, S. M., and S. M. Wu. 1983. *Time Series and System Analysis with Applications*. New York: Wiley.

Park, M., J. Kim, M. K. Jeong, A. M. S. Hamouda, K. N. Al-Khalifa, and E. A. Elsayed. 2012. "Economic Cost Models of Integrated APC Controlled SPC Charts." *International Journal of Production Research* 50 (14): 3936–3955.

Peña, D., G. C. Tiao, and R. S. Tsay. 2011. *A Course in Time Series Analysis*. New York: Wiley.

Shumway, R. H., and D. S. Stoffer. 2010. *Time Series Analysis and Its Applications: With R Examples*. Berlin: Springer Science & Business Media.

Tsung, F., and J. Shi. 1999. "Integrated Design of Run-to-run PID Controller and SPC Monitoring for Process Disturbance Rejection." *IIE Transactions* 31 (6): 517–527.

Tsung, F., H. Wu, and V. N. Nair. 1998. "On the Efficiency and Robustness of Discrete Proportional-integral Control Schemes." *Technometrics* 40 (3): 214–222.

Tsung, F., J. Shi, and C. F. J. Wu. 1999. "Joint Monitoring of PID-controlled Processes." *Journal of Quality Technology* 31: 275–285.

Vander Wiel, S. A. 1996. "Monitoring Processes That Wander Using Integrated Moving Average Models." *Technometrics* 38: 139–151.

Wang, K., and F. Tsung. 2007. "Monitoring Feedback-controlled Processes Using Adaptive T2 Schemes." *International Journal of Production Research* 45 (23): 5601–5619.

Wardell, D. G., H. Moskowitz, and R. D. Plante. 1994. "Run-length Distributions of Special-cause Control Charts for Correlated Processes." *Technometrics* 36 (1): 3–17.